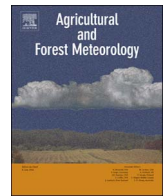




Contents lists available at ScienceDirect

Agricultural and Forest Meteorology

journal homepage: www.elsevier.com/locate/agrformet

Incorporating diffuse radiation into a light use efficiency and evapotranspiration model: An 11-year study in a high latitude deciduous forest

Sheng Wang^{a,*}, Andreas Ibrom^a, Peter Bauer-Gottwein^a, Monica Garcia^{a,b}

^a Department of Environmental Engineering, Technical University of Denmark, 2800 Kgs. Lyngby, Denmark

^b International Research Institute for Climate and Society, The Earth Institute, Columbia University, Palisades, NY, USA

ARTICLE INFO

Keywords:

Diffuse PAR fraction
Eddy covariance
Gross primary production
Evapotranspiration
Top-down
Models
Light use efficiency model
Priestley–Taylor Jet Propulsion Laboratory
evapotranspiration model

ABSTRACT

The fraction of diffuse photosynthetically active radiation (PAR) reaching the land surface is one of the biophysical factors regulating carbon and water exchange between terrestrial ecosystems and the atmosphere. This is especially relevant for high latitude ecosystems, where cloudy days are prevalent. Without considering impacts of diffuse PAR, traditional ‘top-down’ models of ecosystem gross primary productivity (GPP) and evapotranspiration (ET), which use satellite remote sensing observations, are biased towards clear sky conditions. This study incorporated a cloudiness index (CI), an index for the fraction of diffuse PAR, into a joint ‘top-down’ model that uses the same set of biophysical constraints to simulate GPP and ET for a high latitude temperate deciduous forest. To quantify the diffuse PAR effects, CI along with other environmental variables derived from an eleven-year eddy covariance data set were used to statistically explore the independent and joint effects of diffuse PAR on GPP, ET, incident light use efficiency (LUE), evaporative fraction (EF) and ecosystem water use efficiency (WUE). The independent and joint effects of CI were compared from global sensitivity analysis of the ‘top-down’ models. Results indicate that for independent effects, CI increased GPP, LUE, ET, EF and WUE. Analysis of joint effects shows that CI mainly interacted with the radiation intercepted in the canopy (PAR, net radiation and leaf area index) to influence GPP, ET and WUE. Moreover, Ta and vapor pressure saturation deficit played a major role for the joint influence of CI on LUE and EF. In the growing season from May to October, variation in CI accounts for 11.9%, 3.0% and 7.8% of the total variation of GPP, ET and transpiration, respectively. As the influence of CI on GPP is larger than that on ET, this leads to an increase in WUE with CI. Joint GPP and ET model results showed that when including CI, the root mean square errors (RMSE) of daily GPP decreased from 1.64 to 1.45 g C m⁻² d⁻¹ (11.7% reduction) and ET from 15.79 to 14.50 W m⁻² (8.2% reduction). Due to the interaction of diffuse PAR with plant canopies, the largest model improvements using CI for GPP and ET occurred during the growing season and for the transpiration component, as suggested by comparisons to sap flow measurements. Furthermore, our study suggests a potential biophysical mechanism, not considered in other studies: under high diffuse PAR conditions, due to the increased longwave emission from clouds, canopy temperature gets higher and enhances GPP and transpiration in this temperature-limited high latitude ecosystem.

1. Introduction

Quantifying land surface water and carbon fluxes is of critical importance for ecosystem and water resources management. The temporal dynamics of land surface carbon and water fluxes are controlled by the interplay of various biophysical factors, e.g. climate forcing (solar radiation, water vapor and temperature), atmospheric conditions (CO₂ concentration and nitrogen deposition) and biotic factors (leaf area index and plant functional types) (Ciais et al., 2005; Dunn et al., 2007; Wu et al., 2016). Among these biophysical factors, the fraction of

diffuse photosynthetically active radiation (PAR), f_{diff} (the ratio between diffuse and total PAR), has been highlighted to have strong implications for the global carbon cycle (Gu et al., 2003; Mercado et al., 2009). It could increase the efficiency of photosynthesis, which has been referred to the diffuse fertilization effect (Roderick et al., 2001; Kanniah et al., 2012). Further, predictions showed that, at the global scale, aerosols in the atmosphere would increase by 36% in 2100 (Heald et al., 2008). Aerosols influence cloud formation and increase f_{diff} in the atmosphere (Schiermeier, 2006). This is especially important for high latitude ecosystems, which are already exposed to a higher f_{diff}

* Corresponding author.

E-mail address: swan@env.dtu.dk (S. Wang).

<http://dx.doi.org/10.1016/j.agrformet.2017.10.023>

Received 16 July 2017; Received in revised form 10 October 2017; Accepted 17 October 2017

0168-1923/ © 2017 Elsevier B.V. All rights reserved.

Nomenclature*Latin alphabet*

CI	Cloudiness index (dimensionless)
EF	Evaporative fraction (dimensionless)
ET	Evapotranspiration (mm d^{-1})
f_{APAR}	Fraction of absorbed PAR (dimensionless)
f_{ci}	Cloudiness index constraint (dimensionless)
f_{diff}	Fraction of diffuse PAR (dimensionless)
f_{g}	the green canopy fraction indicating the proportion of active canopy (dimensionless)
f_{M}	the plant moisture constraint (dimensionless)
f_{IPAR}	Fraction of intercepted PAR (dimensionless)
f_{Ta}	the air temperature constraint reflecting the temperature limitation of photosynthesis (dimensionless)
f_{SWC}	the soil moisture constraint on photosynthesis (dimensionless)
f_{VPD}	the VPD constraint reflecting the stomatal response to the atmospheric water saturation deficit (dimensionless)
G	Ground heat flux (W m^{-2})
GPP	Gross primary productivity ($\text{g C m}^{-2} \text{d}^{-1}$)
k_{PAR}	the extinction coefficients for PAR (0.5, dimensionless)
k_{Rn}	the extinction coefficients for Rn (0.6, dimensionless)
LAI	Leaf area index ($\text{m}^2 \text{m}^{-2}$)
LUE	Incident light use efficiency (g C MJ^{-1})
LW_{in}	Incoming longwave radiation (W m^{-2})
LW_{out}	Outgoing longwave radiation (W m^{-2})
NDVI	Normalized difference vegetation index (dimensionless)
PAR	Photosynthetically active radiation ($\text{MJ m}^{-2} \text{d}^{-1}$)
PARc	PAR intercepted by the canopy ($\text{MJ m}^{-2} \text{d}^{-1}$)

RH	the relative humidity (dimensionless)
Rn	Net radiation (W m^{-2})
Rnc	Net radiation intercepted by the canopy (W m^{-2})
Rns	Net radiation reaching to the soil (W m^{-2})
SWC	Soil water content ($\text{m}^3 \text{m}^{-3}$)
SW_{in}	Incoming shortwave radiation (W m^{-2})
SZA	Sun zenith angle (rad)
Ta	Air temperature ($^{\circ}\text{C}$)
Ts	Surface temperature ($^{\circ}\text{C}$)
To	Optimal air temperature for vegetation growth ($^{\circ}\text{C}$)
VPD	Vapor pressure deficit (hPa)
WUE	Ecosystem water use efficiency (g C kg^{-1})

Greek alphabet

α	PT coefficient, an empirical ratio of potential evapotranspiration to equilibrium potential evapotranspiration (dimensionless)
γ	the psychrometric constant ($0.066 \text{ kPa } ^{\circ}\text{C}^{-1}$)
Δ	the slope of saturation-to-vapor pressure curve ($\text{kPa } ^{\circ}\text{C}^{-1}$)
ε	Surface emissivity (dimensionless)
ε_{max}	Maximum LUE ($\text{g C m}^{-2} \text{MJ}^{-1}$)
λ	Latent heat of vaporization (kJ kg^{-1})
λET	Latent heat flux of evapotranspiration (W m^{-2})
λEc	Latent heat flux from transpiration (W m^{-2})
λEi	Latent heat flux from evaporation of intercepted water (W m^{-2})
λEs	Latent heat flux from evaporation of soil water (W m^{-2})
σ	the Stefan-Boltzmann constant ($5.670367 \times 10^{-8} \text{ kg s}^{-3} \text{K}^{-4}$)

due to low solar height and high frequency of overcast and cloudy conditions.

With more uniform vertical distribution of incoming photosynthetic active radiation (PAR) under cloudy conditions, both observations and modeling studies have confirmed more active carbon assimilation rates (Gu et al., 2002; Lloyd et al., 2002; Steiner and Chameides, 2005; Ibrom et al., 2006; Urban et al., 2012). However, the gross primary productivity (GPP) enhancement depends on local environmental conditions and ecosystem types. Healy et al. (1998) reported that increasing f_{diff} can increase the incident light use efficiency (LUE, defined as the ratio between GPP and incoming PAR). This increases crop yield by as much as 50% for maize, soybean and peanuts. According to observations from 10 temperate forest flux sites in USA, Cheng et al. (2015) found that f_{diff} explained up to 41% and 17% of seasonal variations in GPP in croplands and forests, respectively. In a modeling study, Ibrom et al. (2006) found the uniform PAR distribution in the maritime Scottish climate with a ca. 20% higher f_{diff} lead to a 13–14% higher LUE compared to the continental climate in Germany in spruce canopies. To identify the impacts of f_{diff} , the covariance of f_{diff} and other environmental factors (Kanniah et al., 2012) should also be taken into account. For instance, Williams et al. (2016) found that without considering the covariance between f_{diff} and phenology, the GPP enhancement from f_{diff} is 260%, while by separating f_{diff} and phenology, the GPP enhancement induced by f_{diff} dropped to 22%. Apart from modeling studies at the global scale (Mercado et al., 2009), few studies have focused on ecosystems in high latitude regions, which are radiation and temperature limited (van Dijk et al., 2005; Lagergren et al., 2008). In these ecosystems, the influence of f_{diff} and its covariance with other environmental variables should be thoroughly quantified, because the potential mechanisms influencing GPP and ET might be different from those of water-limited ecosystems.

Because photosynthesis and transpiration are closely linked via

stomatal behaviors, f_{diff} is expected to also have moderate impacts on land evapotranspiration (ET) and may eventually influence the global hydrological cycle and the climate system (Knohl and Baldocchi, 2008; Davin and Seneviratne, 2012; Pedruzo-Bagazgoitia et al., 2017). For instance, the modeling results from the Community Land Model showed that higher f_{diff} during 1960–1990 increased the latent heat flux of evapotranspiration (λET) in the tropics by 2.5 Wm^{-2} (3% of mean) and reduced global river runoff (Oliveira et al., 2011). By employing the COSMO-CLM2 regional climate model, Davin and Seneviratne (2012) identified f_{diff} could alter the seasonal evaporative fraction (EF, defined as the ratio between λET and available energy, which is net radiation minus soil heat flux Rn-G) and a consistent fraction (up to 3%) of the overall variability in European summer air temperature could be explained by f_{diff} . With increasing f_{diff} , the magnitude of the ET increase due to f_{diff} has been shown to be smaller than that of GPP, resulting in an increase in the ecosystem water use efficiency (WUE, defined as the ratio between GPP and ET) (Knohl and Baldocchi, 2008; Oliveira et al., 2011). Similarly to GPP, the local environment can also alter the responses of ecosystem ET, EF and WUE to f_{diff} . For instance, in temperature-limited ecosystems at high latitudes, incoming longwave radiation has been shown to be an important source of energy for snow and glacier melting under cloudy conditions with high f_{diff} increasing surface temperature (Juszak and Pellicciotti, 2013). However, the impacts of higher longwave radiation on the energy budget and canopy temperature have not been considered yet, despite their potentially important implications for vegetation activities. In general, compared to studies on evaluating impacts of f_{diff} on GPP and LUE, studies on the influence of f_{diff} on ET, EF and WUE are limited. More studies are needed to quantify impacts and understand mechanisms linking f_{diff} to ET, EF and WUE.

Traditionally, models that incorporate satellite remotely sensed observations, e.g. vegetation indices, surface temperature or albedo, to

Download English Version:

<https://daneshyari.com/en/article/6536897>

Download Persian Version:

<https://daneshyari.com/article/6536897>

[Daneshyari.com](https://daneshyari.com)